Modeling aeroacoustic excitations by subsonic wave packets in the Kirchhoff formalism

Romain Serre, Florent Margnat

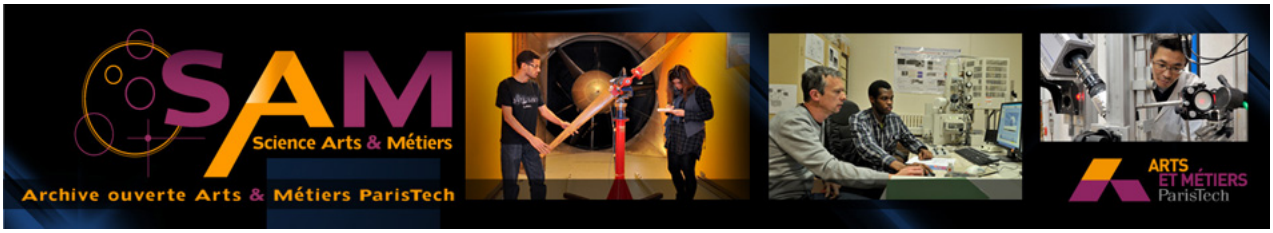

Modeling aeroacoustic excitations by subsonic wave packets in the Kirchhoff formalism

R. Serré[a], F. Margnat[a]

a. *Arts et Métiers ParisTech, DynFluid – 151 Boulevard de l'Hôpital, 75013 Paris, France*

Abstract :

The present work aims at linking the shape of a wave packet to its acoustic efficiency through numerical integration of the homogeneous Helmholtz equation in the Kirchhoff formalism. We shall consider the case of a bidimensional, rectangular domain where one side is affected by a spatially evolving wave packet as a boundary condition with subsonic convection velocity. In the first place, the numerical tool is validated by comparison with analytical developments available in literature. Then, an extension to more advanced forms of wave packet is approached. The appearance of a criterion for acoustic efficiency is discussed, as well as the need for a proper definition regarding the acoustic energy of a wave packet and its radiated energy output.

Résumé :

Le présent travail étudie l'impact de la forme de l'enveloppe spatiale d'un paquet d'ondes sur son efficacité acoustique par le recours à l'outil numérique pour l'estimation de la solution intégrale de l'équation homogène de Helmholtz dans le formalisme de Kirchhoff. Un domaine bidimensionnel et rectangulaire est considéré dont l'un des côtés se voit imposer un paquet d'ondes comme condition limite, convecté à vitesse subsonique. Dans un premier temps, l'outil numérique ainsi élaboré est validé par comparaison avec les résultats analytiques disponibles. Ensuite, une généralisation à d'autres formes d'enveloppes de paquets d'ondes est abordée. L'émergence d'un critère d'efficacité acoustique en fonction du type d'enveloppe est argumentée, tout comme la nécessité d'une définition de l'énergie d'un paquet d'onde et de la puissance acoustique rayonnée.

Keywords : aeroacoustics ; wave packet ; Kirchhoff's integral

1 Introduction

Efforts have been numerous to understand how a wave packet affects the sound field through experimental ([4]), analytical ([1], [3]) and numerical ([1], [2], [5]) research. Laufer & Yen [4] first started to point out experimentally the superdirective character of some acoustic sources in a round jet. Crighton & Huerre [3] stated this feature analytically for some particular forms of the wave packet envelope. Avital & Sandham [1] extended these previous studies to the mixing layer flow. The question has been raised how the envelope of a wave packet influences its acoustic response. In order to reduce mathematical restrictions from analytical developments of Crighton & Huerre [3] and to acquire a more general view on the phenomenon, the problem is approached here in the Kirchhoff formalism. It will give access to the acoustic pressure field depending on the pressure distribution input, namely, the wave packet as boundary condition. This study investigates the effects of wave packets characteristics on their acoustic response. Several envelope forms will be considered. The directivity of the resulting acoustic field is studied as well as an efficiency criterion. The present paper is organised as follow : the theoretical background of the acoustics of a wave packet is presented ; then the Kirchhoff method is introduced ; the main results are shown for several wave packet envelopes in section 4 ; a conclusion is drawn.

2 Theoretical analysis of a wave packet

Analytical developments

The present work is based on a numerical resolution of the model first suggested by Crighton & Huerre [3]. On the lower side of the investigated domain, a wave packet models the aeroacoustic excitation. Under the assumption of a static propagation medium, the monochromatic, bidimensional wave equation drives the pressure fluctuations $p(x_1, x_2)$ of one particular mode

$$\frac{\partial^2 p}{\partial x_1^2} + \frac{\partial^2 p}{\partial x_2^2} + M_c^2 p = 0 \qquad x_1 \in \mathbb{R} \text{ and } x_2 \in \mathbb{R}^+ \tag{1}$$

where M_c is the convection Mach number defined as $M_c = k_{ac}/k_h$ with k_{ac} and k_h being respectively the acoustic and the hydrodynamic wave numbers ; The associated boundary condition is expressed as

$$p(x_1, 0) = A(\varepsilon x_1)\exp(ik_h x_1) \tag{2}$$

where A is the envelope function and i is the imaginary unit. The parameter ε is taken as $\varepsilon = 1/L_{wp}$ as defined by Crighton & Huerre [3], L_{wp} being the wave packet length. Following equation (1) k_h is the reference length ; it will be ignored throughout. Crighton & Huerre [3] showed that a solution of (1) that radiates (2) to infinity can be expressed as

$$p_s(x_1, x_2) = \frac{1}{\varepsilon}\int_{-\infty}^{+\infty} \hat{A}\left(\frac{k-1}{\varepsilon}\right)\exp(ikx_1 - \gamma x_2)\mathrm{d}k \tag{3}$$

with

$$\begin{cases} \gamma = +\sqrt{k^2 - M_c^2} & \text{if} \quad |k| > M_c \\ \gamma = -i\sqrt{M_c^2 - k^2} & \text{if} \quad |k| < M_c \end{cases} \tag{4}$$

where $\hat{A}$ is the Fourier transform of A. From the use of the stationary phase method, which is a far field approximation, one can express equation (3) as

$$p_{an}(r, \theta) \simeq \frac{1}{\varepsilon}\sqrt{\frac{2\pi M_c}{r}}\sin\theta\exp(iM_c r - \frac{1}{4}i\pi)\hat{A}\left(\frac{M_c\cos\theta - 1}{\varepsilon}\right) \tag{5}$$

This simplified model is based on the conditions of a slow spatial variation of the wave packet — namely $\varepsilon = o(1)$ — and a known form of the envelope. Whereas Crighton & Huerre [3] investigated three different envelopes, only the case of the gaussian wave packet is hereby considered for validation purposes for it is found to be the most directive case. Moreover, faster spatial variation of the envelope can be tested with a numerical tool. The properties of the envelope are reminded below :

Spatial envelope ($X = x_1/L_{wp}$)	Spectral envelope ($K = L_{wp}(k-1)$)
$A(X) = \exp[-(X)^2]$	$\hat{A}(K) = \frac{1}{2\sqrt{\pi}}\exp(-\frac{1}{4}K^2)$

Numerical integration

In a low–subsonic flow, one can show from equations (3) and (4) that the main contribution to the sound is given by the wave numbers close to zero. Equation (3) then reduces to

$$p_s(x_1, x_2) \simeq \frac{1}{\varepsilon}\int_{-M_c}^{+M_c} \hat{A}\,(K)\exp(ikx_1 + ix_2\sqrt{M_c^2 - k^2})\mathrm{d}k \tag{6}$$

The integrand in equation (6) is therefore depicted in figure 1a where one can see that the main contribution range is between $-M_c$ and $+M_c$. Additionally, the effect of the spectral integration range on the acoustic pressure is studied with comparison of equation (5). When the spectral integration range goes beneath the range $[-M_c; M_c]$, the error increases dramatically (figure 1b). Some errors still occuring beyond $[-M_c; M_c]$ can be observed in the near field for $R = 5\lambda_{ac}$ (figure 1b). Consequently,

in the following, the spectral domain is reduced to the range $[k_{min}; k_{max}] = [-M_c; M_c]$. For future applications, equation (6) is considered relevant. To find a suitable discretisation step in the spectral domain (namely Δk), a convergence study is carried out. Results are shown in figure 1c for four distance of the directivity arc. When the radius R of the latter exceeds $20\lambda_{ac}$, the error falls below a few percents for $\Delta k \leqslant 10^{-4}$. For smaller R, the far field approximation made in equation (5) leads to an error when decreasing Δk. Figure 1c shows that equation (5) is not accurate in the near field, as expected.

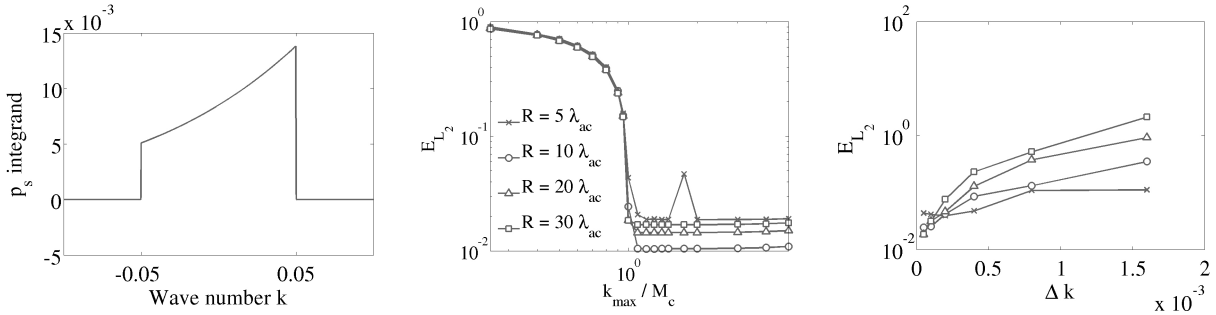

(a) Integrand of p_s. (b) $\frac{\|p_s - p_{an}\|_2}{\|p_{an}\|_2}$ with k_{max}. (c) $\frac{\|p_s - p_{an}\|_2}{\|p_{an}\|_2}$ with Δk.

Figure 1: Main contribution in wave numbers range (left) ; Validation of spectral integration range (centre) ; validation of spectral integration (right). The 2–norm of a vector $\boldsymbol{x}$ defined as $\|\boldsymbol{x}\|_2 = (\sum_{i=1}^{n} |x_i|^2)^{\frac{1}{2}}$ with $x_i = x(\theta_i)$ at a specified radius and $\theta_i \in [0°; 180°]$. $M_c = 0.05$, $L_{wp} = 1/\sqrt{M_c}$.

3 Kirchhoff modeling

Theoretical background

The problem is now modeled by wave extrapolation method in the spectral form of Kirchhoff's formalism. In the observer region of coordinates $\mathbf{x} = (x_1, x_2)$, the pressure fluctuations $p_K(\mathbf{x})$ are expressed as

$$p_K(\mathbf{x}) = \int_\Sigma \left\{ G(\mathbf{x}|\mathbf{y}) \frac{\partial p(\mathbf{y})}{\partial \mathbf{n}} - p(\mathbf{y}) \frac{\partial G(\mathbf{x}|\mathbf{y})}{\partial \mathbf{n}} \right\} \mathrm{d}\Sigma(\mathbf{y}) \tag{7}$$

regarding the pressure fluctuations $p(\mathbf{y})$ as the boundary condition. Here $\Sigma(\mathbf{y})$ is the control surface surrounding the initial pressure distribution of coordinates $\mathbf{y} = (y_1, 0)$ and $\mathbf{n}$ its outward pointing normal. The bidimensional Green's function is considered

$$G(\mathbf{x}|\mathbf{y}) = \frac{i}{4} H_0^{(2)}(M_c r) \underset{r \mapsto +\infty}{\simeq} -\frac{\exp(-iM_c r - i\pi/4)}{\sqrt{8\pi M_c r}} \qquad \text{with} \qquad r = |\mathbf{x} - \mathbf{y}| \tag{8}$$

For computation cost concerns, the far field approximation is used for no difference has been observed from the exact Green's function. Deriving Green's function and assuming the pressure derivative term to be null on the control surface, equation (7) becomes

$$p_K(\mathbf{x}) = \int_{y_2=0} A(y_1/L_{wp}) \left(iM_c + \frac{1}{2r} \right) \frac{(x_2 - y_2)}{r\sqrt{8\pi M_c r}} \exp(iy_1 - iM_c r + i\pi/4) \mathrm{d}y_1 \tag{9}$$

Numerical implementation

This method is applied on the same directivity arcs as before. The numerical step (namely Δy_1) of the wave packet spatial discretisation and the integration length Ly_1 have been investigated for $M_c = 0.05$ and $L_{wp} = 1/\sqrt{M_c}$; these parameters are found to be of minor influence in the observer region though 4 points per hydrodynamic wavelength and a pressure distribution length of $4\lambda_h$ are the minimum required (figures 2a and 2b). Thus, in the following, a numerical step of $\Delta y_1 = \lambda_h/40$ and pressure distribution length of $Ly_1 = 40\lambda_h$ are applied. In figure 2c is presented the good agreement between

the results from equation (6) and the Kirchhoff method through two directivity arcs in the relatively near field. It is thus demonstrated that the system of equations (1) and (2) can be solved with the Kirchhoff formalism.

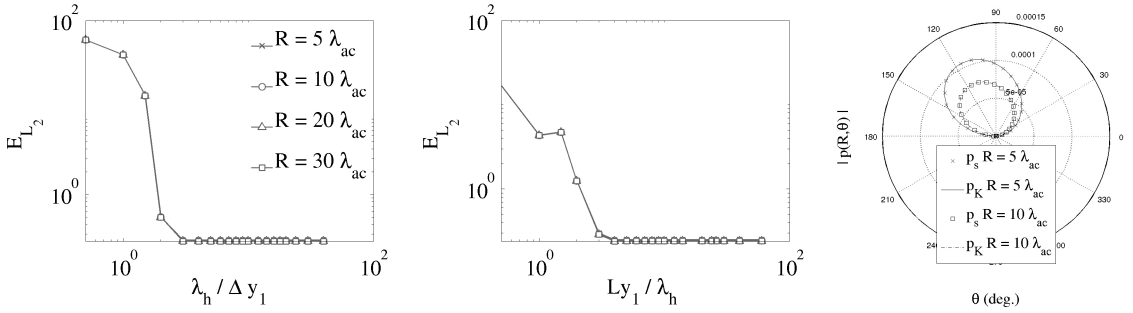

(a) $\frac{\|p_K - p_s\|_2}{\|p_s\|_2}$ with Δy_1. $Ly_1 = 40\lambda_h$. (b) $\frac{\|p_K - p_s\|_2}{\|p_s\|_2}$ with Ly_1. $\Delta y_1 = \frac{\lambda_h}{40}$. (c) Pressure directivity at $5\lambda_{ac}$ and $10\lambda_{ac}$. Comparison between p_s and p_K.

Figure 2: Validation of spatial discretisation (left) ; validation of pressure distribution length (centre) ; validation of the Kirchhoff modeling (right). $M_c = 0.05$, $L_{wp} = 1/\sqrt{M_c}$.

4 Results and discussion

With a validated numerical tool, one can emancipate himself from the reference case situation. The pressure directivity and the acoustic efficiency are presented as a criterion. Through these quantities, effects of spatial deformation are investigated (*e.g.* length or stiffness of the wave packet) and compared with the Mach number effects. Results are thereafter depicted at a radius of $R = 20\lambda_{ac}$ for it is far enough to be considered in the far field, thus avoiding the near field uncertainties highlighted in the preceding section. The directivity arc of distance R is located at the centre of symmetrical wave packets.

Cases' selection

In free shear layers, *e.g.* the mixing layer flow, pressure fluctuations can be seen as a wave packet being convected towards downstream direction as shown by Moser *et al.* [5]. In the latter, one can identifiy spatial characteristics that may impact the associated sound response, as for instance, a different expansion on the upstream and a contraction on the downstream ; that is non symmetrical wave packet. Thus, three main variations from the case of Crighton & Huerre [3] are tested here. Associated equations are stated herebelow with the variable coefficient E and the fixed coefficient σ, both representing the stiffness of the wave packet. Are shown : a Mach number variation from 0.025 to 0.5 (figure 3) ; an upstream expansion of the gaussian wave packet (figure 4) to fit the mixing layer case feature ; a downstream contraction (figure 5) for symmetrical effects. In all cases, two fixed stiffness parameters σ are used to draw attention on the feature being investigated. In the Mach number study, the envelope is symmetrically defined as $A(y_1/L_{wp}) = \exp(-(\sigma y_1/L_{wp})^2)$.

Upstream expansion	Downstream contraction
$y_1 < 0 : A(y_1/L_{wp}) = \exp(-(\frac{E}{L_{wp}}y_1)^2)$	$y_1 < 0 : A(y_1/L_{wp}) = \exp(-(\frac{\sigma}{L_{wp}}y_1)^2)$
$y_1 > 0 : A(y_1/L_{wp}) = \exp(-(\frac{\sigma}{L_{wp}}y_1)^2)$	$y_1 > 0 : A(y_1/L_{wp}) = \exp(-(\frac{E}{L_{wp}}y_1)^2)$

Acoustic pressure and directivity

Following results are organised to show from left to right, the wave packet envelope for two fixed stiffness parameters (σ), the pressure directivity and the angle of maximum pressure in the directivity range.

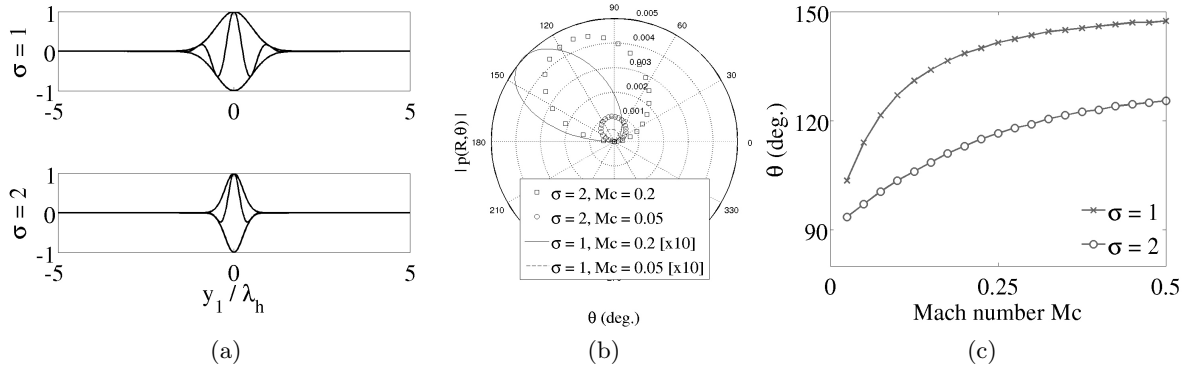

(a) (b) (c)

Figure 3: Mach number variation. Crighton & Huerre [3] results recovered for $M_c = 0.05$. $L_{wp} = 1/\sqrt{0.05}$.

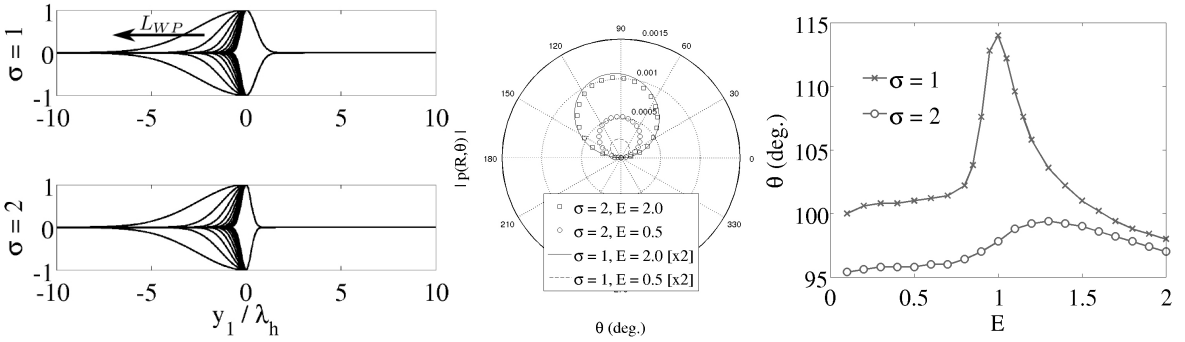

(a) (b) (c)

Figure 4: Upstream expansion of the envelope. $M_c = 0.05$. $L_{wp} = 1/\sqrt{0.05}$.

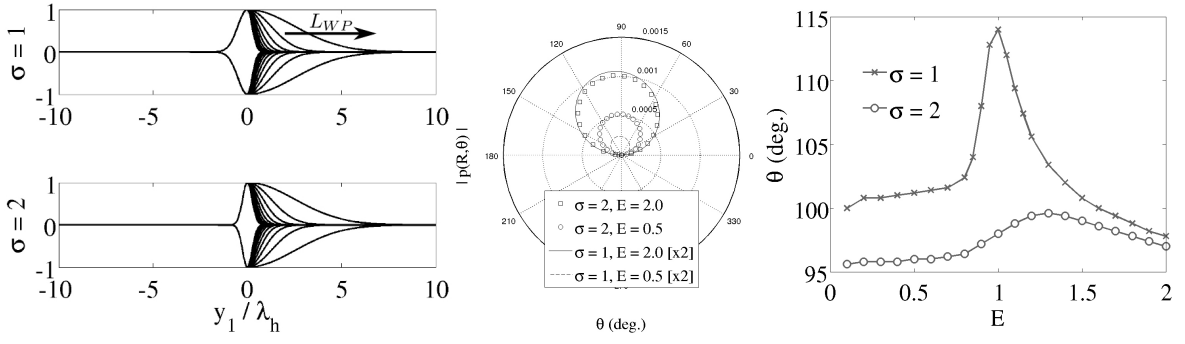

(a) (b) (c)

Figure 5: Downstream contraction of the envelope. $M_c = 0.05$. $L_{wp} = 1/\sqrt{0.05}$.

What first come in mind of one looking at the previous results, is the strong Mach number influence on maximum pressure level and directivity regardless of the stiffness coefficient. But the latter has more importance. Pressure level is 10 times higher when σ is doubled. With a higher stiffness coefficient, the directivity has a lower magnitude (figures 3b and 3c). An upstream expansion or a downstream contraction produce the same effect. The direction to which the wave packet is stretched has no significant effect. Expansion or contraction both reduce softly the pressure level, although this feature is emphasized when σ is increased. With the latter two configurations, the directivity oscillates around a particular value with a high peak when $E = 1$. As opposed to what happens with the pressure level, the peak is weakened when σ is increased.

Acoustic efficiency

Acoustic efficiency is defined as the ratio between the power provided as input from the wave packet and the power radiated as output from the associated acoustic response of the latter. These quantities

are expressed as

$$W_i = \int_{y_2=0} \frac{\mathcal{R}e\left\{p(y_1,0)\right\}^2}{\rho_0 c_0 M_c} \mathrm{d}y_1 \quad ; \quad W_o = R\int_0^{\pi} \frac{\mathcal{R}e\left\{p_K(R,\theta)\right\}^2}{\rho_0 c_0} \mathrm{d}\theta \tag{10}$$

W_i and W_o respectively stand for the total acoustic power input and ouput ; The former being integrated over the directivity arc of radius R. The acoustic efficiency is then defined as $\eta = W_o/W_i$ and plotted in figure 6 fot the three cases.

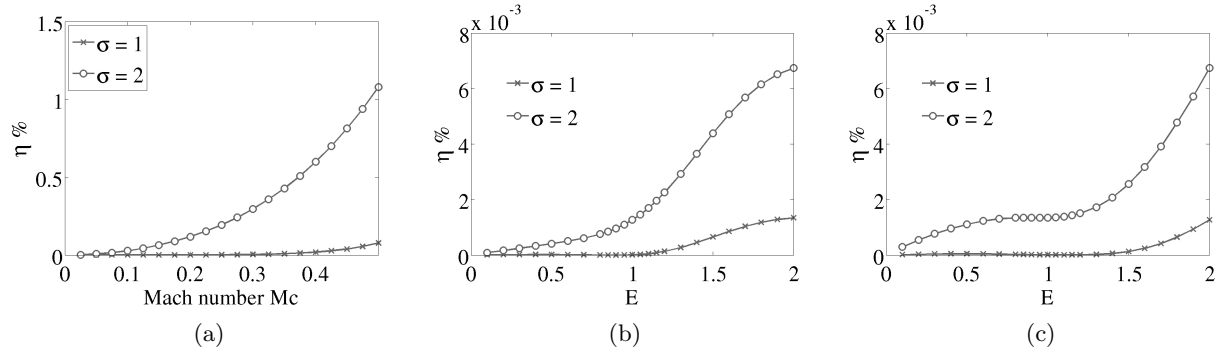

Figure 6: Acoustic efficiency η at $20\lambda_{ac}$. From left to right : Mach variation ; upstream expansion for $M_c = 0.05$; downstream contraction for $M_c = 0.05$. $L_{wp} = 1/\sqrt{0.05}$.

The Mach number first appears to be the most efficient parameter. One may notice the efficiency is amplified and almost reaches 110%. Consequently, equation (10) is an efficiency and not a performance. Combined with the stiffness, efficiency is strongly amplified. But computations for either spatial expansion or contraction of the envelope were carried out at a Mach number $Mc = 0.05$. According to figure 6a, efficiency does not exceed 9.10^{-6}% and 7.10^{-3}% ($\sigma = 1$ and $\sigma = 2$ respectively) for such a Mach number value while in both cases of spatial deformation, efficiency reaches 1.10^{-3}% and 7.10^{-3}%. Stretching a wave packet envelope with a low σ provide more efficient results than increasing the Mach number. For higher σ, stretching is not found to be efficient enough compared to the Mach number effect.

5 Conclusions

From the present results, one main conclusion is that the Mach number has significant impact on pressure level and directivity but less on efficiency, except when combined with stiffness. This conclusion is to be soften though, when put aside the spatial deformation study carried out in the present paper. Wave packet envelope functions are clearly a major parameter driving the energetic response and directivity of a wave packet. It has been highlighted what are the most predominant features. Furthermore, the side whose the wave packet is extended, whether upstream or downstream is of no major effects and shows a symmetrical behavior.

6 Acknowledgement

Authors thank Professor J.–C. Robinet for helpful discussions.

References

[1] Avital, E.J., Sandham, N.D., Luo, K.H. 1998 Mach wave radiation by mixing layers. Part I: analysis of the sound field. *Theoret. Comput. Fluid Dynamics* **12** 73–90

[2] Cavalieri, A.V.G., Jordan, P., Agarwal, A., Gervais, Y. 2011 Jittering wave–packet models for subsonic jet noise. *J. Sound and Vibration* **330** 4474–4492

[3] Crighton, D.G., Huerre, P. 1990 Shear-layer pressure fluctuations and superdirective acoustic sources. *J. Fluid Mech.* **220** 355–368

[4] Laufer, J., Yen, T.C. 1983 Noise generation by a low Mach number jet. *J. Fluid Mech.* **134** 1-32.

[5] Moser C., Lamballais E., Margnat F., Fortuné V., Gervais Y. 2012 Numerical study of Mach number and thermal effects on sound radiation by a mixing layer. *International Journal of Aeroacoustics* **11** 555.